International Journal of Engineering & Technology, 4 (1) (2015) 61-70
www.sciencepubco.com/index.php/IJET

doi: 10.14419/ijet.v4i1.3965
Research Paper

Numerical simulation of air–water two–phase flow in vertical pipe using k-ε model

Ali Sanati

Faculty of Petroleum and Petrochemical Engineering, Hakim Sabzevari University, Sabzevar, Iran
E-mail: sanatiam@gmail.com

Abstract

Two-phase flow exists mostly in pipes and is of substantial importance in pipeline industry. Numerical data are presented in this paper for water and air velocity in two-phase flow through vertical circular channel using both K-ε model and empirical correlations. In order to investigate the pressure distribution for various flow conditions, two-phase flow was considered through two vertical pipes with different lengths and the same diameters. Moreover, we studied flow entering from below and getting out from top of the pipe. Results obtained in this study have been analyzed with experimental data, showing that the average void fraction rises with increasing inlet gas velocity and drops with increasing inlet water velocity. Also results show that Hassan & Kabir method is the most appropriate approach in comparison with the others.

Keywords: *Air-Water Two-Phase Flow; Empirical Correlation; K-E Model; Pressure Drop; Vertical Pipe.*

1. Introduction

Two-phase flow in vertical pipe, are commonly used in many applications such as: petroleum industry, food processing, chemical industry, power plants like coal fired power plant and heat transferring of fluids. Two-phase flow and pressure distribution through the pipe have been studied numerically and experimentally by many researchers [1-4]. Cho et al. [1] numerically analyzed the transient two-phase flow in nuclear reactor components, a three- dimensional thermal hydraulics code, named COPID. The simulation result showed that it can reproduce the important characteristics of the downcomer boiling, such as a flow pattern change from a bubbly flow to churn and mist flows and a circulation of liquid accelerated by bubbles. Zhao and Bi [2] investigated experimentally two-phase flow in vertical miniature triangular channels, effect of hydraulic diameter and Reynolds number on gas velocity, void fraction and pressure drop. Ohnuki and Akimoto [3] studied experimentally flow pattern and phase distribution in air-water two-phase flow along a large vertical pipe, no large bubbles were observed in the region L/D<20 which corresponds to the developing region of the axial differential pressure curves. The large coalescent bubbles were generated in L/D>20.
In this paper, we will consider differential pressure under different inlet gas and liquid velocities using different methods, numerically (K − ε model (mixture approach)) and with empirical correlations (Duns and Ros [7], Orkiszewski [8], Hasan & Kabir [25-27] and Mukherjee & Brill [28]). Then we'll compare the results with experimental data and the appropriate method will be determined.

2. Methods

2.1. Pressure gradient

The pressure-gradient equation derived for single-phase flow can be modified for multiphase flow by considering the fluids to be a homogeneous mixture [20]. Thus,

$$\left(\frac{dP}{dL}\right)_{Tottal} = \left(\frac{dP}{dL}\right)_{friction} + \left(\frac{dP}{dL}\right)_{static} + \left(\frac{dP}{dL}\right)_{acceleration} \quad (1)$$

$$\frac{dP}{dL} = \frac{f\rho_f v_f^2}{2d} + \rho_S . g + \rho_S . v_f \frac{dv_f}{dL} \quad (2)$$

The pressure-drop component caused by friction losses requires evaluation of a two-phase friction factor. The pressure drop caused by elevation change depends on the density of the two-phase mixture which is usually calculated with Eq. 3.

$$\rho_{mix} = \rho_g . \alpha + \rho_L (1 - \alpha) \quad (3)$$

The pressure-drop component caused by acceleration is normally negligible and is considered only for cases of high flow velocities.

2.2. Flow patterns

Predicting the flow pattern that occurs at a given location in a well is extremely important. The empirical correlation or mechanistic model used to predict flow behavior varies with flow pattern. Essentially all flow-pattern predictions are based on data from low-pressure systems, with negligible mass transfer between the phases and with a single liquid phase. These flow patterns, shown schematically in Fig. 1. Slug and churn flow are sometimes combined into a flow pattern called intermittent flow. It is common to introduce a transition between slug flow and annular flow that incorporates churn flow.

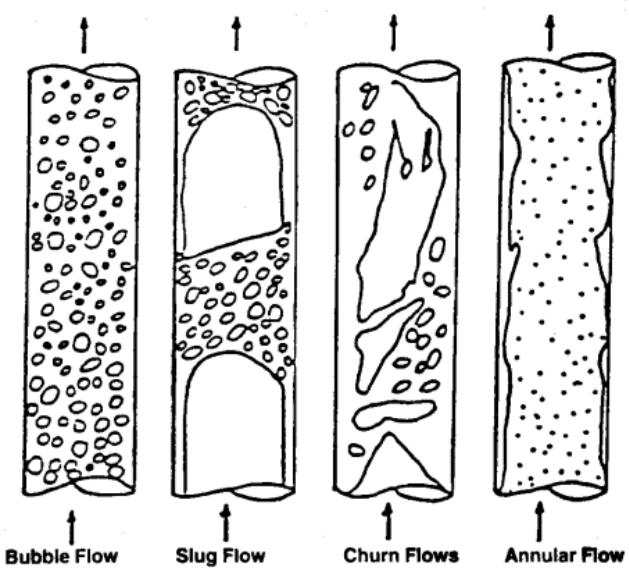

Fig. 1: Upward Vertical Flow Patterns

2.3. Pressure-gradient prediction

The methods used to predict pressure gradient can be classified as empirical correlations and computational method.

2.4. Empirical correlations

Empirical correlations used in this paper, are based on Duns and Ros [7], Orkiszewski [8], Hasan & Kabir [25-27] and Mukherjee & Brill [28] method. All Theses correlations require liquid holdup, friction factor and flow pattern to be determined.

2.4.1. Duns and Ros empirical correlation

Duns and Ros method is a result of an extensive laboratory study in which liquid holdup and pressure gradients were measured. Liquid holdup was measured by use of a radioactive-tracer technique. For each of three flow patterns observed, correlations were developed for friction factor and slip velocity, from which liquid holdup could be calculated [7].

2.4.1.1. Flow-pattern prediction

Fig. 2 shows the flow-pattern map developed by Duns and Ros. The flow-pattern transition boundaries are defined as functions of the dimensionless groups, namely, N_{gv} andN_{Lv}.

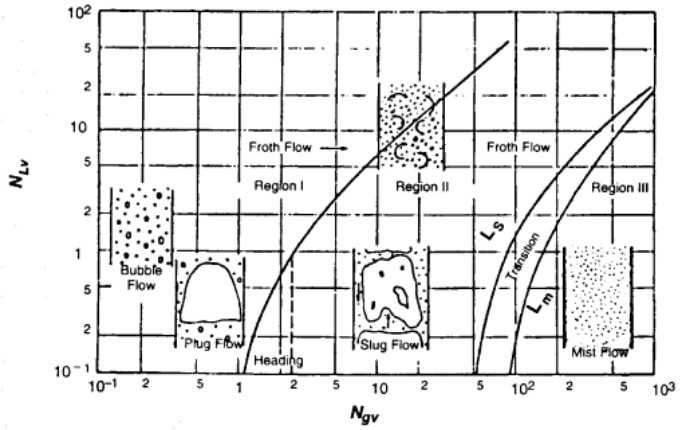

Fig. 2: Duns And Ros Flow-Pattern Map.

2.4.1.2. Liquid-holdup prediction

Duns and Ros developed empirical correlations for a dimensionless slip-velocity number and defined holdup as follows,

$$H_L = \frac{v_s - v_m + \sqrt{(v_m - v_s)^2 + 4 v_s v_{sL}}}{2\, v_s} \quad (4)$$

$$v_s = v_g - v_L \quad (5)$$

$$v_m = v_{sg} + v_{sL} \quad (6)$$

$$v_{sL} = \frac{q_L}{A_p}, v_{sg} = \frac{q_g}{A_p} \quad (7)$$

$$\rho_s = \rho_L H_L + \rho_g (1 - H_L) \quad (8)$$

The friction pressure-gradient component for bubble and slug flow is given by,

$$\left(\frac{dP}{dL}\right)_f = \frac{f\, \rho_L v_{sL} v_m}{2\, d} \quad (9)$$

Also for mist flow is given by,

$$\left(\frac{dP}{dL}\right)_f = \frac{f\, \rho_g v_{sg}^2}{2\, d} \quad (10)$$

2.4.2. Orkiszewski empirical correlation [8]

Orkiszewski selected what he considered to be the most accurate correlation for bubble and mist flow and proposed a new correlation for slug flow. This slug-flow correlation was developed with Hagedorn and Brown [6] data. Orkiszewski selected the Griffith and Wallis [10, 11] method for bubble flow and Duns and Ros [7] method for mist flow.

2.4.2.1. Flow-pattern prediction

Orkiszewski used Duns and Ros flow-pattern transition for the boundaries between slug and mist flow, including the transition region between them. For boundary between bubble and slug flow, he chose criteria established by Griffith and Wallis.

$$\lambda_{g_{B/S}} = L_B \quad (11)$$

$$L_B = 1.071 - 0.2218 \frac{v_m^2}{d} \quad (12)$$

$$H_L = 1 - \frac{1}{2}\left[1 + \frac{v_m}{v_s} - \sqrt{(1 + \frac{v_m}{v_s})^2 - 4\frac{v_{sg}}{v_s}}\right] \quad (13)$$

Bubble Flow:

$$\boldsymbol{\lambda_g = \frac{q_g}{q_g + q_L} \leq \lambda_{g_{B/S}}} \quad (14)$$

$$\boldsymbol{\left(\frac{dP}{dL}\right)_f = \frac{f \rho_L (\frac{v_{sL}}{H_L})^2}{2\, d}} \quad (15)$$

Slug Flow:

$$\boldsymbol{\lambda_g = \frac{q_g}{q_g + q_L} \geq \lambda_{g_{B/S}}} \quad (16)$$

$$\left(\frac{dP}{dL}\right)_f = \frac{f\, \rho_L v_m^2}{2\, d}\left[\left(\frac{v_{sL} + v_b}{v_m + v_b}\right) + \Gamma\right] \quad (17)$$

$$\Gamma = \frac{0.013\, log\, \mu_L}{d^{1.38}} - 0.287 - 0.162\, log v_m - 0.428\, log\, d$$

$$v_b = C_1 C_2 \sqrt{g\, d}$$

2.4.3. Hasan and Kabir Method [25-27]

2.4.3.1. Flow-pattern prediction

To model flow-pattern transition, Hasan and Kabir identified the same four flow patterns shown in Fig. 1.

$$v_{sg} = \frac{sin\theta}{4-C_o}(C_o v_{sL} + v_s) \quad (18)$$

C_o Is the flow coefficient given by Eq. 19?

$$C_o = \begin{cases} 1.2 \; if \; d < 0.12 \; m \quad or \; if \; v_{sL} > 0.02 \; m/s \\ 2.0 \; if \; d > 0.12 \; m \quad or \; if \; v_{sL} < 0.02 \; m/s \end{cases} \quad (19)$$

For the transition to dispersed-bubble flow, Taitel et al. [23] proposed

$$v_m^{1.12} = 4.68 \; d^{0.48} \left[\frac{g(\rho_L - \rho_g)}{\sigma_L}\right]^{0.5} \left(\frac{\sigma_L}{\rho_L}\right)^{0.6} \left(\frac{\rho_L}{\mu_L}\right)^{0.08} \quad (20)$$

2.4.3.2. Flow-behavior prediction

Total pressure gradient in two-phase flow can be written as the sum of the gravitation or hydrostatic $(dp/dL)_{el}$, friction $(dp/dL)_f$, and acceleration $(dp/dL)_{acc}$ component. Thus,

$$(\frac{dP}{dL})_{Tottal} = (\frac{dP}{dL})_{el} + (\frac{dP}{dL})_f + (\frac{dP}{dL})_{acc} \; = \rho_s \; g \; sin\theta + \frac{f v_m^2 \rho_s}{2d} + \rho_s v_m \frac{dv_m}{dL} \quad (21)$$

Where

$$\rho_s = \rho_g(1 - H_L) + \rho_L H_L \quad (22)$$

In general, the acceleration component can be neglected.

In bubble and dispersed-bubble flow the expression for holdup, H_L is

$$H_L = 1 - \frac{v_{sg}}{C_o v_m + v_s} \quad (23)$$

$$v_s = 0.35 \left(gd \frac{\rho_L - \rho_g}{\rho_L}\right)^{0.5} \sqrt{sin\theta}(1 + cos\theta)^{1.2} \quad (24)$$

To estimate total pressure gradient, Eq. 21 can be used with the mixture density calculated from liquid holdup estimated with Eq. 23. Estimation of the friction component presents some difficulty, because some liquid flows downward in a film around the Taylor bubbles, while most of liquid flows upward in the liquid slug. Wallis [24] suggested that the wall shear stress around the vapor bubble should be ignored. With this assumption, the friction pressure gradient becomes:

$$\left(\frac{dp}{dL}\right)_f = \frac{f v_m^2 \rho_L H_L}{2d} \quad (25)$$

2.4.4. Mukherjee and brill method [28]

2.4.4.1. Flow-pattern prediction

For flow-pattern observations and measuring liquid holdup, they used air and kerosene or lube oil. Approximately 1000 pressure-drop measurements and more than 1500 liquid-holdup measurements were obtained for a broad range of gas and liquid flow rates.

$$N_{Lv_{B/s}} = 10^x \quad (26)$$

Where

$$x = log \; N_{gv} + 0.94 + 0.074 \; sin\theta - 0.855 \; sin^2\theta + 3.69 \; N_L$$

$$N_{gv_{S/M}} = 10^{(1.401 - 2.694 N_L + 0.521 N_{Lv}^{0.329})} \quad (27)$$

In downflow and horizontal flow, the bubble/slug transition is described by

$$N_{gv_{B/S}} = 10^y \quad (28)$$

Where

$$y = 0.431 - 3.003 \; N_L - 1.138(log \; N_{Lv}) sin\theta - 0.429(log \; N_{Lv})^2 \; sin\theta + 1.132 sin\theta$$

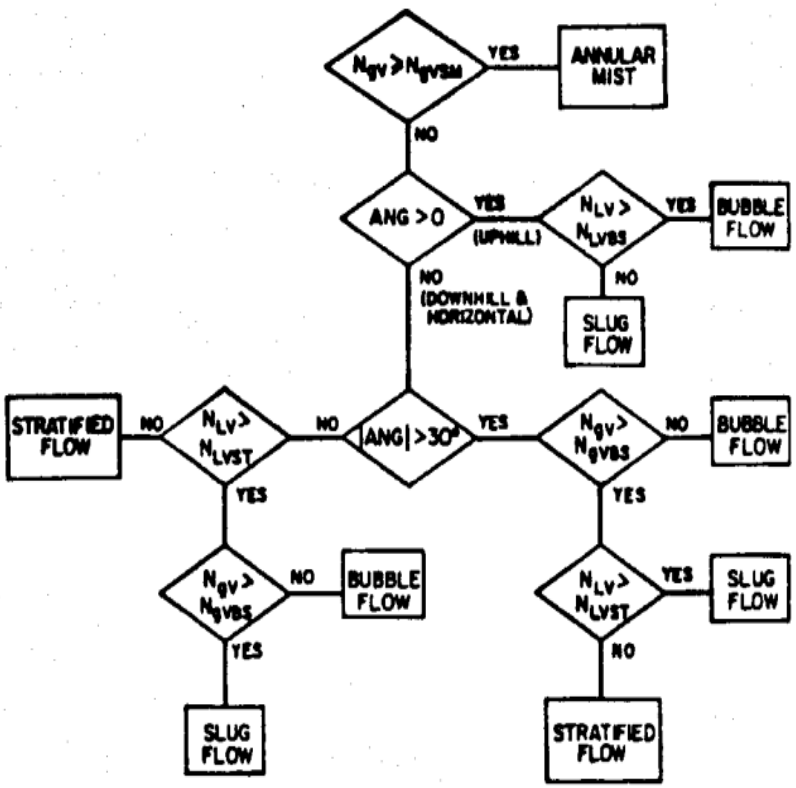

Fig. 3: Flow Chart to Predict Flow Patterns by Use of the Flow-Pattern Transition Equations.

2.4.4.2. Liquid-holdup prediction

The liquid-holdup data were correlated with an equation of the form

$$H_L = exp\left[(C_1 + C_2 sin\theta + C_3 sin^2\theta + C_4 N_L^2)\left(\frac{N_{gv}^{C_5}}{N_{Lv}^{C_6}}\right)\right] \quad (29)$$

Bubble and Slug Flow:
The pressure gradient for bubble flow and slug flow is determined from

$$\frac{dp}{dL} = \frac{\frac{f\rho_s v_m^2}{2d} + \rho_s\, g\, sin\theta}{1 - E_k} \quad (30)$$

Where

$$E_k = \frac{\rho_s v_m v_{sg}}{p} \quad (31)$$

Annular Flow:
The pressure gradient for annular flow is determined from Eq. 31 and

$$\frac{dp}{dL} = \frac{\frac{f\rho_n v_m^2}{2d} + \rho_s\, g\, sin\theta}{1 - E_k} \quad (32)$$

2.5. Numerical model

2.5.1. Original k − ε model

The K-epsilon model is one of the most common turbulence models. It is a two equation model that means, it includes two extra transport equations to represent the turbulent properties of the flow. This allows a two equation model to account for history effects like convection and diffusion of turbulent energy. The first transported variable is turbulent kinetic energy, k. The second transported variable in this case is the turbulent dissipation, ε. The $k - \varepsilon$ Model Equations are,
For Turbulent Kinetic Energy:

$$\frac{\partial}{\partial t}(\rho k) + \frac{\partial}{\partial X_i}(\rho k u_i) = \frac{\partial}{\partial X_j}\left[\left(\mu + \frac{\mu_t}{\sigma_k}\right)\frac{\partial k}{\partial X_j}\right] + P_k + P_b - \rho\varepsilon - Y_m + S_k \quad (33)$$

For Dissipation:

$$\frac{\partial}{\partial t}(\rho \varepsilon) + \frac{\partial}{\partial X_i}(\rho \varepsilon u_i) = \frac{\partial}{\partial X_j}\left[\left(\mu + \frac{\mu_t}{\sigma_\varepsilon}\right)\frac{\partial \varepsilon}{\partial X_j}\right] + C_{1\varepsilon}\frac{\varepsilon}{k}(P_k + C_{3\varepsilon}P_b) - C_{2\varepsilon}\rho\frac{\varepsilon^2}{k} + S_\varepsilon \quad (34)$$

$$P_k = -\rho\overline{u_i' u_j'}\frac{\partial u_j}{\partial x_i} \quad (35)$$

$$P_k = \mu_t S^2 \quad (36)$$

S is the modulus of the mean rate-of-strain tensor defined as,

$$S = \sqrt{2\, S_{ij} S_{ij}} \quad (37)$$

P_b is the effect of buoyancy which has been neglected in this subject.

Turbulent viscosity is modeled as,

$$\mu_t = \rho \varepsilon_\mu \frac{k^2}{\varepsilon} \quad (38)$$

Model Constants,

$C_{1\varepsilon} = 1.44$, $C_{2\varepsilon} = 1.92$, $C_{3\varepsilon} = 0.09$, $\sigma_k = 1.0$, $\sigma_\varepsilon = 1.3$

2.5.1.1. Mixture approach [22]

The average equations of multiphase flow can be written in numerous ways. Equations can be derived by time averaging, space averaging, or by any combination of these. In all these methods, the resulting equations contain basically the same terms.

2.5.1.1.1. Continuity equation for the mixture

The continuity equation for k phase is:

$$\frac{\partial}{\partial t}\sum_{k=1}^{n}(\alpha_k \rho_k) + \nabla.\sum_{k=1}^{n}(\alpha_k \rho_k v_k) = \sum_{k=1}^{n}\Gamma_k \quad (39)$$

Γ Is the rate of mass transfer (kg/$m^3.s$). Because the total mass is conserved, the right hand side of Eq. (46) must be vanished,

$$\sum_{k=1}^{n}\Gamma_k = 0 \quad (40)$$

And we obtain the continuity equation of the mixture

$$\frac{\partial \rho_m}{\partial t} + \nabla.(\rho_m v_m) = 0 \quad (41)$$

Here the mixture density and the mixture velocity are defined as

$$\rho_m = \sum_{k=1}^{n}\alpha_k \rho_k \quad (42)$$

$$v_m = \frac{1}{\rho_m}\sum_{k=1}^{n}\alpha_k \rho_k v_k \quad (43)$$

Equation (48) has the same form as the continuity equation for single phase flow. If the density of each phase is a constant and the interphase mass transfer is excluded, the continuity equation for the mixture is

$$\nabla.\sum_{k=1}^{n}\alpha_k v_k = 0 \quad (44)$$

2.5.1.1.2. Momentum equation for the mixture

The continuity equation for k phase is:

$$\frac{\partial}{\partial t}\sum_{k=1}^{n}(\alpha_k \rho_k v_k) + \nabla.\sum_{k=1}^{n}(\alpha_k \rho_k v_k v_k) = -\sum_{k=1}^{n}\alpha_k \nabla p_k + \nabla.\sum_{k=1}^{n}\alpha_k(\tau_k + \tau_{Tk}) + \sum_{k=1}^{n}\alpha_k \rho_k\, g + \sum_{k=1}^{n}M_k \quad (45)$$

Using the definitions (49) and (50) of the mixture density ρ_m and the mixture velocityv_m, the second term of (52) can be rewritten as

$$\nabla.\sum_{k=1}^{n}\alpha_k\, \rho_k\, v_k\, v_k = \nabla.(\rho_m\, v_m\, v_m) + \nabla.\sum_{k=1}^{n}\alpha_k\, \rho_k\, v_{Mk}\, v_{Mk} \quad (46)$$

Where, v_{Mk} is the diffusion velocity, the velocity of phase k relative to the center of the mixture mass.

$$v_{Mk} = v_k - v_M \quad (47)$$

M_k Is the average interfacial momentum source for phase k and τ_k is the average viscous stress tensor.

2.5.2. Numerics

In the present work, the single phase $k-\varepsilon$ model (Launder and Spalding, 1974) was extended to multiphase flows by appropriately accounting for the volume fraction of the phases. The equations were discretized using the finite-volume method. The simulation program could use the second-order upwind discretization scheme (Melaaen, 1992).

2.5.3. Velocity field

The superficial gas and liquid velocities, j_G and j_L and the mean gas and liquid phase velocities, U_G and U_L are defined, respectively, as

$$j_G = \frac{Q_G}{A_p} \quad , \quad j_L = \frac{Q_L}{A_p} \quad (48)$$

$$U_G = \frac{j_G}{\alpha} \quad , \quad U_L = \frac{j_L}{1-\alpha} \quad (49)$$

$$j_{mix} = \frac{\rho_g.j_g.\alpha + j_L.\rho_L.(1-\alpha)}{\rho_{mix}} \quad (50)$$

$$\alpha = \frac{Q_g}{Q_g + Q_L} \quad (51)$$

$$H = \frac{Q_L}{Q_L + Q_g} \quad (52)$$

$$\alpha + H = 1 \quad (53)$$

In above considerations, since the length of the pipe is not so long, superficial velocities mean velocities and inlet velocities have been approximated equally.

3. Results

3.1. Flow pattern

Prediction of flow pattern based on Duns and Ros [7] (Fig. 2), Orkiszewski [8] (Eq. 11-16), Hasan & Kabir [25-27] and Mukherjee & Brill [28] method considered and results can be observed in table 1. Table 1 show that Ork. Method has approximately different result in flow pattern in comparison with three other methods (Duns & Ros, Hasan & Kabir, and Mukherjee & Brill).

Table 1: Ork. Method Which Has Approximately Different Result in Flow Pattern in Comparison with Three other Methods (Duns & Ros, Hasan & Kabir, Mukherjee & Brill).

Length of pipe =12.3 m					
Velocity (m/s)		Flow Pattern			
$j_L\ (\frac{m}{s})$	$j_g\ (\frac{m}{s})$	Duns & Ros Method	Ork. Method	Hasan & Kabir Method	Mukherjee & Brill Method
0.18	0.03	Bubble	Slug	Bubble	Bubble
0.18	0.83	Slug	Bubble	Slug	Slug
0.18	2	Slug	Bubble	Slug	Slug
0.18	4.7	Slug	Bubble	Slug	Slug
1.06	0.03	Bubble	Bubble	Bubble	Bubble
1.06	0.26	Bubble	Bubble	Bubble	Bubble
1.06	0.83	Bubble	Bubble	Slug	Slug
1.06	3.1	Slug	Bubble	Slug	Slug

3.2. Differential pressure

Fig. 4, 5 show the differential pressure in vertical pipe (L=12.3m) under the inlet various velocities in different methods. Also Fig. 6 shows the mean error of different methods with respect to experimental data [3]. The void fraction is a function of gas and liquid velocity increasing with rising gas velocity and decreasing with rising the liquid velocity. This affects Eq. 3 and changes the mixture density. Increasing gas velocity, according to Eq. 48, causes gas volume flow rate to increase. Eq. 52 shows that increasing gas volume flow rate subsequently leads to reduce the holdup (H_L). So, total density (Eq. 22) which depends on holdup, reduces due to the fact that $\rho_L > \rho_g$ and also because $\rho_L H_L$ is affected more compared to$\rho_g H_L$. Finally, based on Eq. 2, rising gas velocity accompanies with differential pressure decrease (pressure drop). Knowing that hydrostatic pressure loss is more than that of frictional pressure loss, reduction of gas velocity or rising of liquid velocity will lead to opposite result, i.e. they result in rise of pressure (pressure drop). As mentioned before, rising gas velocity causes holdup to reduce. Also according to Eq. 53, reduction of holdup will increase void fraction (α), i.e. accelerating gas velocity will increase void fraction. Since$\rho_g < \rho_L$, in vertical flows directing upward, gas moves faster and this causes the volume occupied by gas to increase and void fraction subsequently increases. Based on explanations in the preceding paragraphs, rise of void fraction causes a decrease in differential pressure. Therefore, in two-phase upward vertical flows, increasing the height will be accompanied by reduction in differential pressure. The flow below the height of nearly 4m is not developed and this causes to nonlinear relationship between the elevation and differential pressure, so at the height of 4m, a peak of differential pressure is observed which is clear from the experimental data. Fig. 6 depicts that Hasan & Kabir method is the best method compared to the others. In the second case, the boundary conditions of the problem have been changed. In this case, the length of pipe has been considered 24m, the same amount for which Shen et al. [4] have worked according to experimental condition. This time, gas velocity is constant and liquid velocity changes like the previous situation. As a result, pressure decreases along the flow direction, but pressure difference corresponding to the total length of pipe also increases. This fact is apparent in Fig. 7.

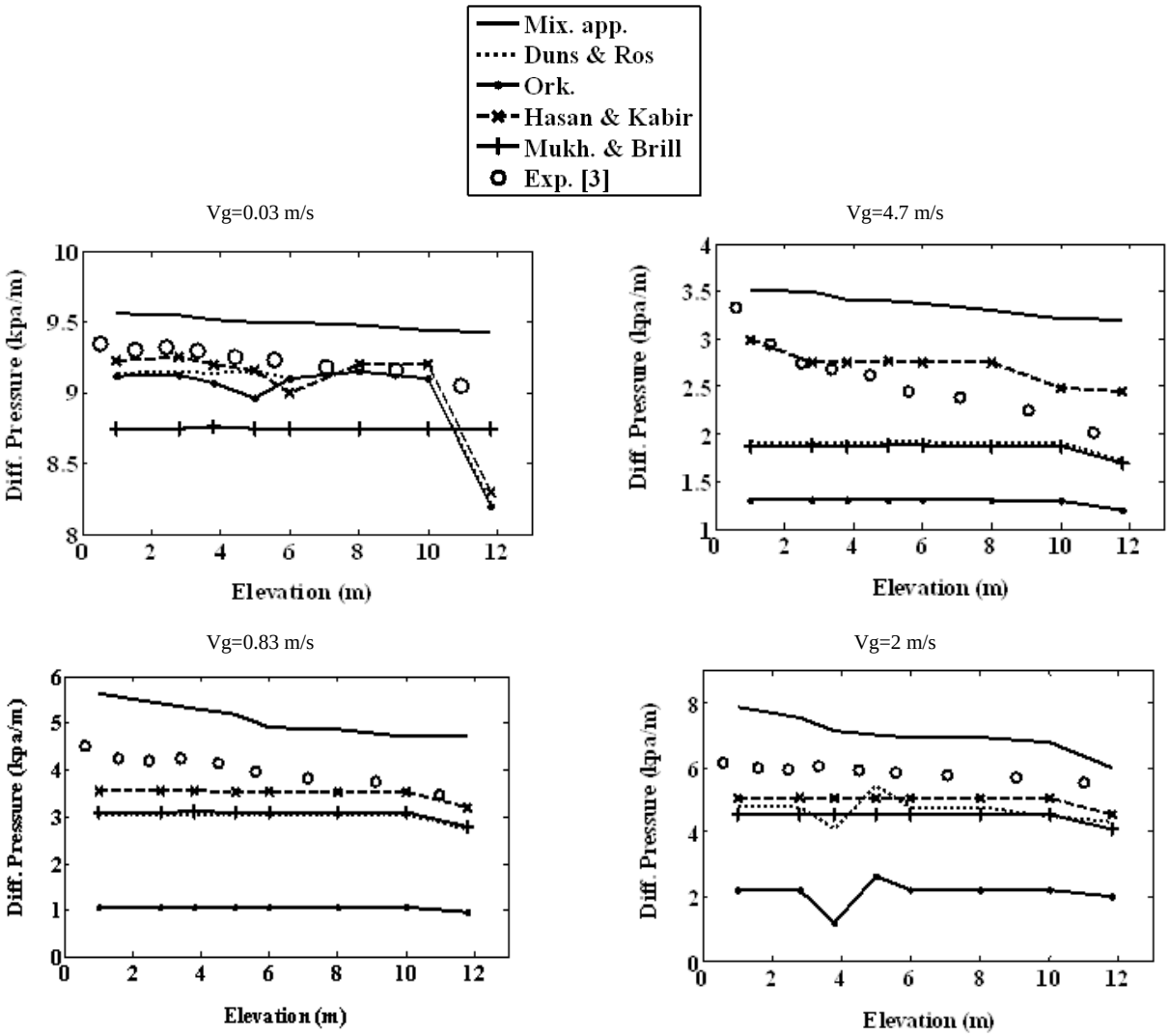

Fig. 4: Comparison of Differential Pressure in Different Methods. (V_L = 0.18 M/S, Length of Pipe=12.3 M).

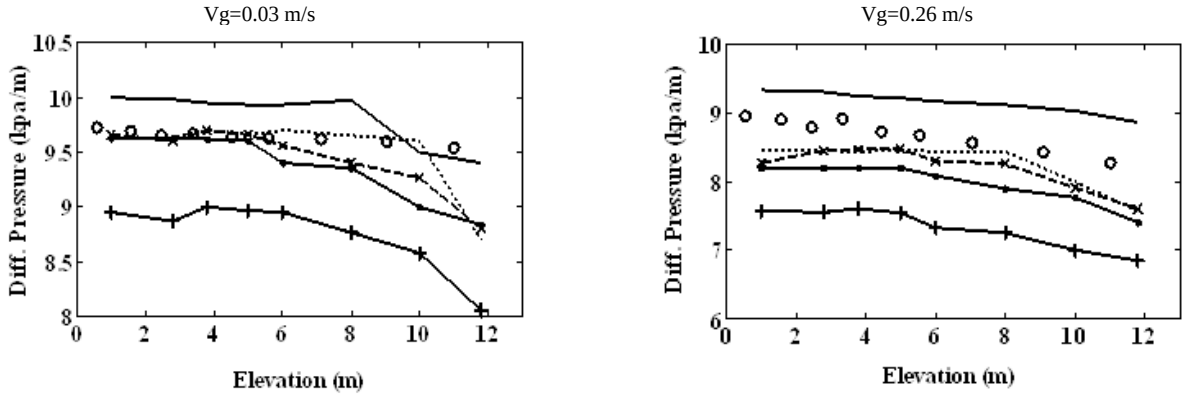

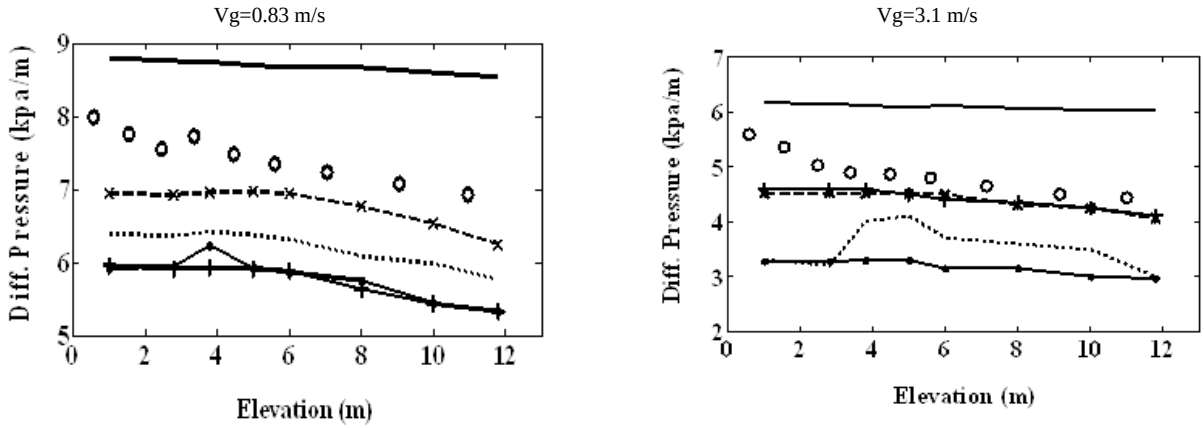

Fig. 5: Comparison of Differential Pressure in Different Methods. ($V_L = 1.06$, Length of Pipe=12.3 M).

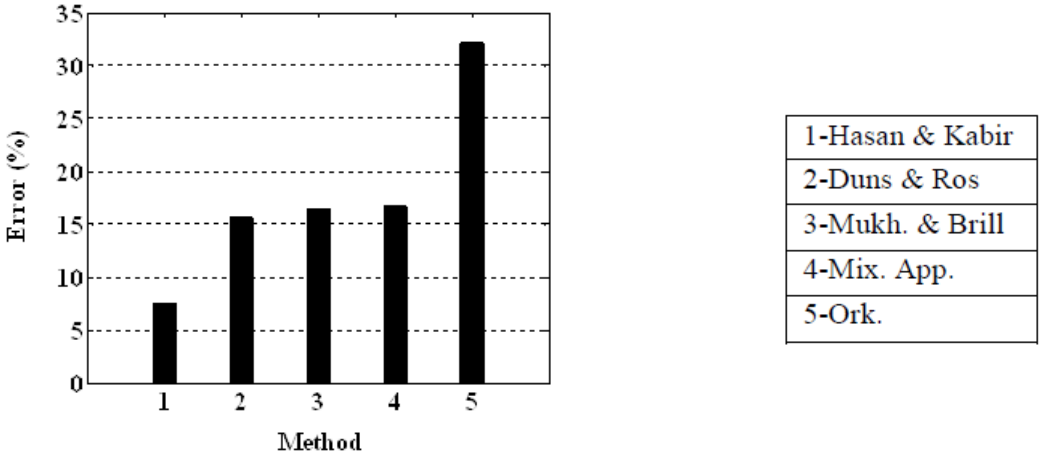

Fig. 6: Mean Error With Respect to Experimental Data [3]. ($V_L = 0.18, 1.06$, Length of Pipe=12.3 M)

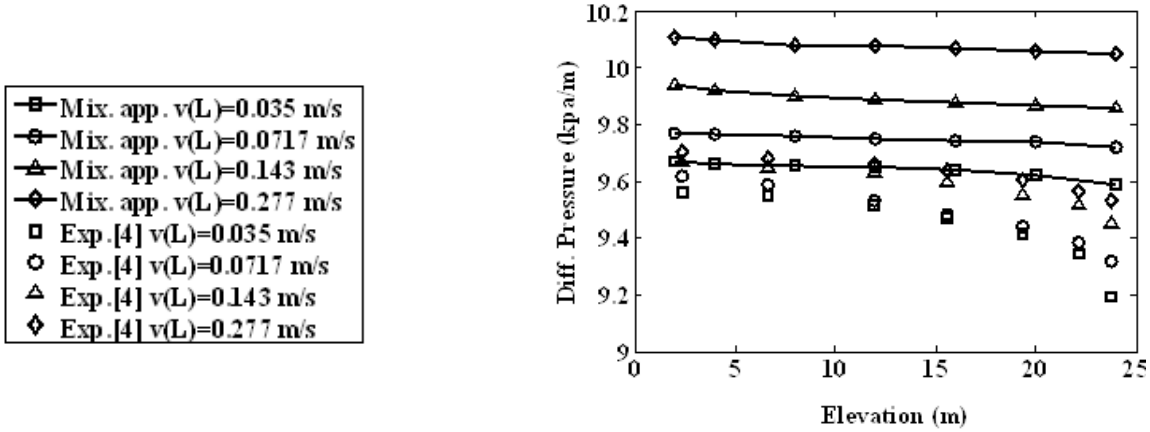

Fig. 7: Comparison of Differential Pressure in Different Liquid Velocities. ($V_G = 0.0311$ M/S, Length of Pipe =24 M)

4. Discussion

Two-phase flow was studied in two vertical pipes having different lengths under different velocities. Flow pattern was considered with the Duns and Ros [7], Ork. [8], Hasan & Kabir [25-27] and Mukherjee & Brill [28] methods. According to flow pattern results, Ork. Method has approximately different result in comparison with three other methods (Duns & Ros, Hasan & Kabir, and Mukherjee & Brill), and Then the variation of pressure along flow direction was investigated in vertical pipe. Considering upward two-phase flow, we analyzed variation of this pressure loss with respect to different inlet velocities. Increasing gas velocity was accompanied with increasing of void fraction which subsequently reduced total pressure loss in pipe. On the contrary, increasing liquid velocity was followed by reducing the void fraction and this led to increasing of total pressure loss in pipe. The results achieved were compared to those obtained from experimental studies which figures show their good agreement. Also from figures, it is clear that Hasan & Kabir method is the best compared to others since its results is close to those obtained experimentally.

References

[1] H.K.Cho, B.Jo Yun, H.Y.Yoon and J.J.Jeong, 2011. Assessment of the Two-Phase Flow Models in the CUPID Code Usingg the Downcomer Boilingg Experiment. Jour. of Nuclear Science and Technology.

[2] T.S. Zhao, Q.C. Bi. 2000. Pressure Drop Characteristics of Gas-Liquid Two-Phase Flow in Vertical Miniature Triangular Channels. The Hong Kong University of Science and Technology.

[3] A. Ohnuki, H. Akimoto, 2000. Experimental Study on Transition of Flow Pattern and Phase Distribution in Upward Air-Water Two-Phase Flow along a Large Vertical Pipe. Japan Atomic Energy Research Institute, 319-1195.

[4] X.Shen, K.Mishima, H.Nakamura, 004. Two-Phase Phase Distribution in a Vertical Large Diameter Pipe. International Jour. of Heat and Mass Transfer. 48 211-225.

[5] K.A. Ibrahim, M.A. El-Kadi, Mofren H. Hamed and Samy M. El-Behery, 2006. Gas-Solid Two-Phase Flow in 90o Bend. Alexandria Eng. Journal. 417-433.

[6] Hagedorn, A.R. and Brown, K.E. Experimental Study of Pressure Gradients Occurring During Continuous Two-Phase Flow in Small-Diameter Vertical Conduits. JPT (April 1965) 475; Trans. AIME, 234.

[7] Duns, H. Jr. and Ros, N.C.J. Vertical Flow of Gas and Liquid Mixtures in Wells. Proc. Sixth World Pet. Cong. Tokyo (1963) 451.

[8] Orkiszewski, J. Prediction Two-Phase Pressure Drops in Vertical Pipes. JPT (June 1967) 829; Trans. AIME, 240.

[9] Taitel, Y.M., Barnea, D., and Dukler, A.E. Modeling Flow Pattern Transitions for Steady Upward Gas-Liquid Flow in Vertical Tubes. AICHE J. (1980) 26, 345. http://dx.doi.org/10.1002/aic.690260304.

[10] Griffith, P. and Wallis, G.B. Two-Phase Slug Flow. J. Heat Transer. (August 1961) 83, 307. http://dx.doi.org/10.1115/1.3682268.

[11] Griffith, P. Two-Phase Flow in Pipes. Special Summer Program, Masschusetts Inst. of Technology, Cambridge, Massachusetts (1962).

[12] Brill, J.P. and Beggs, H.D. Two-Phase in Pipes, U. of Tulsa, Tulsa, Oklahoma (1991).

[13] Beggs, H.D. and Brill, J.P. A Study of Two-Phase Flow in Inclined Pipes. JPT (May 1973) 607; Trans. AIME, 255.

[14] Davies, R.M. and Taylor, G. The Mechanics of Large Bubbles Rising Through Extended Liquids and Through Liquids in Tubes, Proc., Royal Soc. London (1949) 200A, 375.

[15] Brill, J.P. Discontinuities in the Orkiszewski Correlation for Predicting Pressure Gradients in Wells. J. Energy Res. Tech. (March 1989) 111, 34. http://dx.doi.org/10.1115/1.3231398.

[16] Bardina, J.E., Huang, P.G., Coakley, T.J. (1997), "Turbulence Modeling Validation, Testing, and Development", NASA Technical Memorandum 110446.

[17] Jones, W. P., and Launder, B. E. (1972), "The Prediction of Laminarization with a Two-Equation Model of Turbulence", International Journal of Heat and Mass Transfer, vol. 15, 1972, pp. 301-314. http://dx.doi.org/10.1016/0017-9310(72)90076-2.

[18] Launder, B. E., and Sharma, B. I. (1974), "Application of the Energy Dissipation Model of Turbulence to the Calculation of Flow Near a Spinning Disc", Letters in Heat and Mass Transfer, vol. 1, no. 2, pp. 131-138. http://dx.doi.org/10.1016/0094-4548(74)90150-7.

[19] Wilcox, David C (1998). "Turbulence Modeling for CFD". Second edition. Anaheim: DCW Industries, 1998. pp. 174.

[20] P. Brill and H. Mukherjee. 1999. Multiphase Flow in Wells.

[21] T. J. Chung. 2002. Computational Fluid Dynamics.

[22] Mikko Manninen and Veikko Taivassalo. 1996. on the Mixture Model for Multiphase Flow.

[23] Taitel, Y. M, Barnea, D., and Dukler, A. E. 1980. Modeling Flow Pattern Transitions for Steady Upward Gas-Liquid Flow in Vertical Tubes. AIChE J. 26,345. http://dx.doi.org/10.1002/aic.690260304.

[24] Wallis, G.B. 1969. One Dimensional Two-Phase Flow. McGraw-Hill Book Co. Incm, New York City.

[25] Hasan, A.R. and Kabir, C.S. May 1988. A Study of Multiphase Flow Behavior in Vertical Wells, SPEPE 263; Trans., AIME, 285.

[26] Hasan, A.R. and Kabir, C.S. November 1988. Predicting Multiphase Flow Behavior in a Deviated Well, SPEPE 474.

[27] Kabir, C.S. and Hasan, A.R. 1990. Performance of a Two-Phase Gas/Liquid Model in Vertical Wells. J. Pet. Sci & Eng. 4,273.

[28] Mukherjee, H. and Brill, J.P. December 1985. Pressure Drop Correlations for Inclined Two-Phase Flow, J. Energy Res. Tech. 107,549. http://dx.doi.org/10.1115/1.3231233.